JOURNAL OF NATURAL PRODUCTS

pubs.acs.org/jnp

Article

Ormosianines A−P, Structurally Diverse Quinolizidine Alkaloids with AChE Inhibitory Effects from *Ormosia yunnanensis*

Qiong Jin,[#] Xu-Jie Qin,[#] Wen-Jie Sun, Xiao Ding, Yun Zhao, Chang-Bin Wang, Xing-Yu Tao, and Xiao-Dong Luo*

Cite This: *J. Nat. Prod.* 2023, 86, 2193−2205

Read Online

ACCESS | Metrics & More | Article Recommendations | Supporting Information

ABSTRACT: Sixteen new quinolizidine alkaloids (QAs), named ormosianines A−P (**1**−**16**), and 18 known congeners (**17**−**34**) were isolated from the stems and leaves of *Ormosia yunnanensis*. The structures were elucidated based on spectroscopic analyses and electron circular dichroism (ECD) calculations. Structurally, ormosianines A (**1**) and B (**2**) are the first examples of cytisine and *Ormosia*-type alkaloids with the cleavage of the piperidine ring. Results of the acetylcholinesterase (AChE) inhibitory assay revealed that the pentacycline *Ormosia*-type QAs, including **1**, **16**, **24**, and **27**−**29**, are good AChE inhibitors. Ormosianine A (**1**) exhibited more potent AChE inhibitory activity with an IC_{50} value of 1.55 μM. Molecular docking revealed that **1** might bind to the protein 1DX4, forming two hydrogen bonds with residues SER-238 and HIS-480.

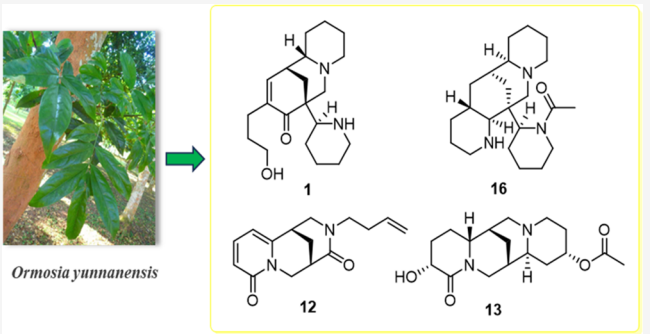

The genus *Ormosia* (Fabaceae family) comprises around 150 species geographically distributed in the humid tropical and subtropical regions of Asia and Australasia.[1] Owing to their nitrogen-fixing properties, approximately 20% of the leguminous plants produce nitrogen-containing secondary metabolites.[2] Quinolizidine alkaloids (QAs) are the characteristic constituents of the *Ormosia* tribe. These alkaloids are biosynthesized from L-lysine[3] and subjected to oxidative cyclization to form the QA skeleton, a chiral bispiperidine core (3,7-diazabicyclo[3.3.1]nonane),[4] substituted by piperidines, pyrrolidines, N-fused 2-pyridones, or α-allyl groups.[5] Quinolizidine alkaloids are an efficient defense against a wide array of predators, physiologically poisonous to herbivores and insects.[6−8] For insects, acetylcholinesterase (AChE) is essential for life. Inhibition of AChE by carbamate or organophosphorus insecticides can be fatal.[9,10] However, extensive use of the market-available insecticides to control insect pests has led to the occurrence of resistant enzymes or insect resistance.[11] Bitter seeds of leguminous plants are naturally toxic to insects, partially due to the presence of QA alkaloids.[12] In our search for structurally intriguing natural products with insect resistance and antimicrobial properties,[13−16] *Ormosia yunnanensis*, a species previously not investigated, was selected for a chemical study. As a result, 16 previously undescribed QAs, ormosianines A−P (**1**−**16**), comprising five distinct types with a varied number of piperidine rings, along with 18 known analogs (**17**−**34**), were isolated and identified. Compounds **1**, **4**, **6**, **11**−**13**, **16**, **24**, and **27**−**29** effectively reversed antiacetylcholinesterase effects with IC_{50} values ranging from 1.55 to 29.6 μM. The underlying interactions between selected bioactive compounds (**1**, **12**, **13**, and **16**) and AChE (1DX4) were predicted via molecular docking studies. The isolation, structural elucidation, AChE inhibitory effects, and molecular docking of these isolates are described herein.

Ormosianine A (**1**) was isolated as a white powder. The molecular formula, $C_{20}H_{32}N_2O_2$, was deduced from its HRESIMS data (*m*/*z* 333.2537 $[M + H]^+$, calculated for 333.2537), indicating six degrees of unsaturation. The UV maximum absorptions at λ_{max} 222 and 245 nm were assigned to a conjugated carbonyl group, whereas the IR absorptions implied the presence of −OH/−NH (3434 cm^{-1}) and carbonyl/olefinic (1637 and 1445 cm^{-1}) functionalities. The ^1H NMR spectrum (Table 1) displayed a signal for one olefinic proton at δ_H = 6.80 (1H, d, *J* = 7.0 Hz, H-17). The ^{13}C NMR and HSQC spectra (Table 1) indicated 20 carbon signals assigned to a carbonyl group (δ_C 202.9, C-11), one quaternary carbon (δ_C 49.5, C-9), one double bond (δ_C 142.8, C-16; 146.1, C-17), three methines (δ_C 63.6, C-6; 36.2, C-7; 61.1, C-18), and 13 methylenes. The aforementioned data of **1** are

Received: June 8, 2023
Published: August 17, 2023

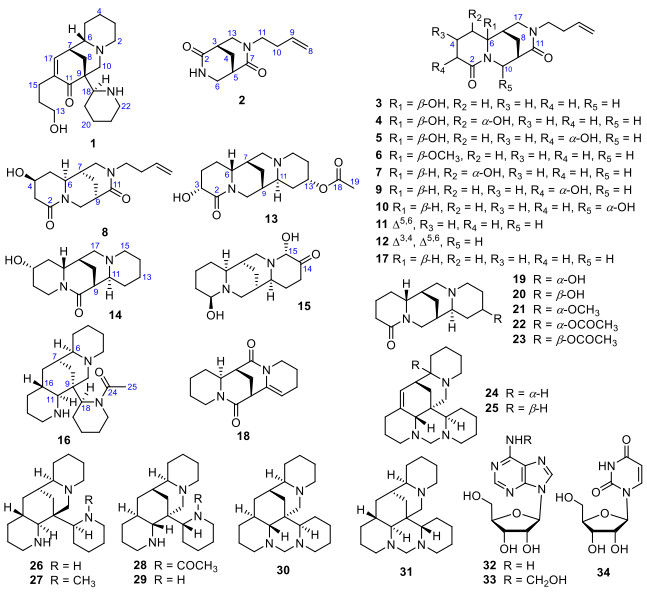

Table 1. ^{13}C (150 MHz) and ^{1}H (600 MHz) NMR Data for 1 in $CDCl_3$

no.	δ_C, type	δ_H (mult., J in Hz)
2	46.5, CH_2	3.35, m
		2.78, m
3	23.5, CH_2	1.95, overlap
		1.80, m
4	23.6, CH_2	1.70, brs
		1.70, brs
5	24.2, CH_2	1.48, overlap
		1.19, m
6	63.6, CH	1.92, m
7	36.2, CH	2.48, brs
8	28.4, CH_2	2.49, m
		2.25, dt (13.6, 6.3)
9	49.5, C	
10	62.1, CH_2	2.72, m
		2.07, d (10.4)
11	202.9, C	
13	62.2, CH_2	3.67, m
14	31.7, CH_2	1.72, brs
		1.61, m
15	33.4, CH_2	2.59, d (12.5)
		1.63, m
16	142.8, C	
17	146.1, CH	6.80, d (7.0)
18	61.1, CH	3.28, m
19	24.6, CH_2	1.48, dt (12.9, 2.8)
		1.19, m
20	25.0, CH_2	1.45, dt (15.9, 5.6)
		1.17, m
21	30.5, CH_2	1.59, m
		1.18, m
22	55.9, CH_2	2.65, d (11.4)
		1.97, m

similar to those of homopodopetaline (**25**)[17] and 6-epihomopodopetaline (**26**).[18] However, the absence of a nitrogen atom (N-2) and a methylidene-nitrogenous unit in **1** as well as the presence of an extra ketone carbonyl (δ_C 202.9, C-11) and an oxygen-bearing methylene (δ_C 62.2, C-13) indicated that **1** was an *Ormosia* alkaloid featuring a *seco*-sparteine combined with a piperidine moiety.

The planar structure of **1** was established by analysis of its 2D NMR spectra (Figure 1). The presence of an α,β-

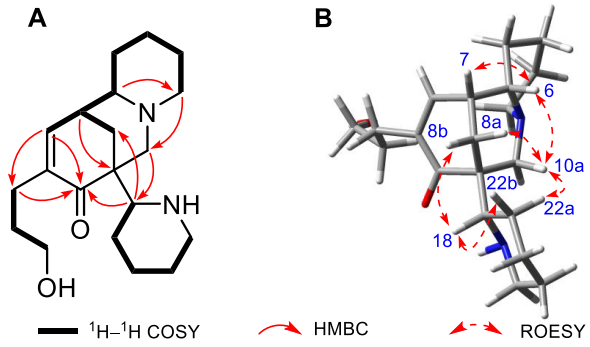

Figure 1. Key (A) ^{1}H–^{1}H COSY, HMBC, and (B) ROESY correlations of **1**.

unsaturated ketone at C-9 was confirmed by the key HMBC corrections from H-17 (δ_H 6.80) to C-11 (δ_C 202.9)/C-6 (δ_C 63.6) and from H-18 (δ_H 3.28) to C-11 (δ_C 202.9)/C-9 (δ_C 49.5). Likewise, a combination with the consecutive ^{1}H–^{1}H COSY (Figure 1A) correlations of H_2-13 (δ_H 3.67)/H_2-14 (δ_H 1.72, 1.61)/H_2-15 (δ_H 2.59, 1.63), the observed correlations from H-17 to C-6 (δ_C 63.6) and C-15 (δ_C 33.4), and correlations from H_2-14 to C-13 (δ_C 62.2)/C-16 (δ_C 142.8) in the HMBC spectrum (Figure 1A) indicated that an *n*-propyl alcohol fragment was located at C-16. Inspection of its HMBC and COSY spectra further indicated that compound **1** shared the same planar structure as that of homopodopetaline. The ROESY correlations (Figure 1B) of H-6 (δ_H 1.92)/H-7 (δ_H 2.47), H-6/H-10a (δ_H 2.72), and H-10a/H-8a (δ_H 2.49)/H-22a (δ_H 2.66) indicated that these hydrogens were β-oriented. In contrast, the ROESY correlations between H-18 (δ_H 3.28)/H-8b (δ_H 2.25) and H-18/H-22b (δ_H 1.97) indicated these hydrogens to be α-oriented. With the aid of an electronic circular dichroism (ECD) calculation (Figure 4), the absolute configuration of compound **1** was assigned as (6*S*,7*R*,9*R*,18*S*).

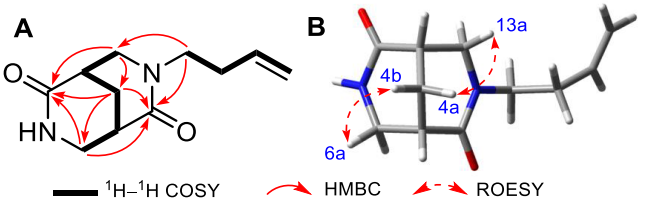

Figure 2. Key (A) ^{1}H–^{1}H COSY, HMBC, and (B) ROESY correlations of **2**.

Ormosianine B (**2**) was obtained as a colorless oil. Its molecular formula ($C_{11}H_{16}N_2O_2$) was defined by analysis of the HRESIMS peak at m/z 209.1282 $[M + H]^+$ (calcd for $C_{11}H_{17}N_2O_2$, 209.1285). The IR spectrum of **2** exhibited the presence of NH (3434 cm^{-1}), carbonyl (1639 cm^{-1}), and olefinic (1496 cm^{-1}) functionalities. The ^{1}H NMR spectrum (Table 2) displayed signals for one terminal olefin at δ_H 5.74 (1H, dt, J = 17.2, 7.0 Hz, H-9), 5.05 (1H, dq, J = 17.1, 1.6 Hz, H-8a), and 5.01(1H, dt, J = 10.2, 1.1 Hz, H-8b). The ^{13}C NMR spectrum (Table 2) displayed 11 carbon signals assigned to two carboxyl groups [δ_C 172.4 (C-2) and 169.7 (C-7)], one

https://doi.org/10.1021/acs.jnatprod.3c00493
J. Nat. Prod. 2023, 86, 2193−2205

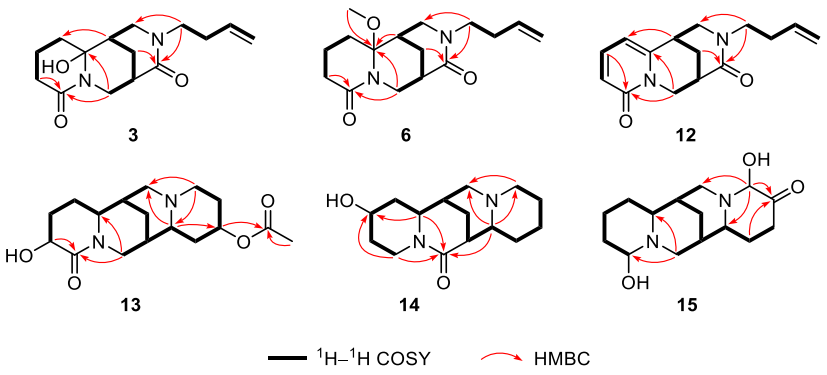

Figure 3. Key ^{1}H−^{1}H COSY and HMBC correlations of compounds **3**, **6**, and **12**−**15**.

double bond [δ_C 117.1 (C-8) and 134.8 (C-9)], five methylene groups [δ_C 25.3 (C-4), 46.7 (C-6), 31.5 (C-10), 45.9 (C-11), and 51.8 (C-13)], and two methines [δ_C 36.2 (C-3) and 36.7 (C-5)]. The above NMR data suggested that compound **2** was structurally similar to tetrahydro-11-oxorhombifoline (**17**),[19] except for the absence of three methylenes and one methine. These data suggested that **2** possessed an elimination of the A-ring of tetrahydro-11-oxo-methicoline. In the HMBC spectrum (Figure 2A), diagnostic correlations from H_2-4 (δ_H 2.12) to C-2 (δ_C 172.4)/C-6 (δ_C 46.7)/C-7 (δ_C 169.7)/C-13 (δ_C 51.8) disclosed the presence of the diazabicyclo[3.3.1]nonane-2,6-dione skeleton. Along with the consecutive ^{1}H−^{1}H COSY correlations (Figure 2A) of H_2-8 (δ_H 5.05, 5.01)/H-9 (δ_H 5.74)/H_2-10 (δ_H 2.31, 2.29)/H_2-11 (δ_H 3.42), the key HMBC correlations from H_2-11 to C-7 (δ_C 169.7)/C-9 (δ_C 134.8)/C-13 (δ_C 51.8) indicated the occurrence of a butadiene fragment placed at N-12. The ROESY cross-peaks (Figure 2B) of H-4a (δ_H 2.12)/H-13a (δ_H 3.54) and H-4b (δ_H 2.12)/H-6a (δ_H 3.54) indicated that two piperidones share a methylene bridge with β-orientation.[19] The absolute configuration of **2**, (3*S*,5*S*), was established by similar profiles of the experimental and calculated ECD spectra (Figure 4).

Ormosianine C (**3**) was isolated as a colorless oil. Its molecular formula of $C_{15}H_{22}N_2O_3$ was determined by the ion peak at *m*/*z* 279.1699 [M + H]$^+$ (calcd for $C_{15}H_{23}N_2O_3$, 297.1703) in the HRESIMS. Analysis of the NMR spectra (Table 3) indicated that compound **3** is an analogue of tetrahydro-11-oxorhombifoline (**17**),[19] bearing an additional hydroxyl group. The HMBC correlations (Figure 3) from H-7 (δ_H 2.11) to C-5 (δ_C 16.1)/C-6 (δ_C 84.3) and from H_2-10 (δ_H 4.45, 3.09) to C-2 (δ_C 171.1)/C-6 (δ_C 84.3) implied that the hydroxyl group was placed at the C-6. ROESY correlations (Figure S2, Supporting Information) of H-8a (δ_H 1.85)/H-10a (δ_H 4.45) and H-8b (δ_H 1.84)/H-7 (δ_H 2.11)/H-13a (δ_H 4.99) indicated that these hydrogens are cofacial, and they were assigned randomly as β-oriented, while the ROESY cross-peaks of H-13b (δ_H 5.70)/H-10b (δ_H 3.09) indicated the α-orientation of these hydrogens. The absolute configuration of **3** was finally elucidated as (6*S*,7*S*,9*S*) by the ECD calculation method (Figure 4).

Ormosianine D (**4**) presented the molecular formula $C_{15}H_{22}N_2O_4$ based on its HRESIMS data (*m*/*z* 293.1507 [M − H]$^-$, calcd for $C_{15}H_{21}N_2O_4$, 293.1507). The NMR data (Table 3) indicated that compound **4** had the same parent skeleton as that of **3**, except for the presence of one more hydroxyl group at C-5. This was substantiated by key HMBC correlations (Figure S1, Supporting Information) from H-7 (δ_H 2.32) to C-5 (δ_C 66.6)/C-6 (δ_C 84.8), as well as correlations from H_2-10 (δ_H 4.11, 2.93) to C-6 (δ_C 84.8) and C-2 (δ_C 169.6), suggesting that two hydroxyl groups were substituted at C-5 and C-6 in **4**, respectively. Additionally, the discernible correlations of H-10a (δ_H 4.11)/H-7 (δ_H 2.32), H-8b (δ_H 1.77)/H-9 (δ_H 2.43), H-8b/H-7, H-8a (δ_H 2.25)/H-5 (δ_H 3.89), and H-8a/H-10a observed in the ROESY spectrum (Figure S2, Supporting Information) of **4** indicated that H-5, H-7, H-8, and H-9 were β-oriented. The absolute configuration of **4** was assigned as (5*S*,6*R*,7*S*,9*S*), on the basis of the calculated ECD analysis (Figure S3, Supporting Information).

Ormosianine E (**5**) presented the same molecular formula of $C_{15}H_{22}N_2O_4$ (*m*/*z* 293.1506 [M − H]$^-$) as that of **4**. Its NMR spectra (Table 3) closely resembled those of **4**, indicating that compounds **5** and **4** are isomeric. HMBC correlations (Figure S1, Supporting Information) from H_2-10 (δ_H 4.42, 3.12) to C-6 (δ_C 85.3)/C-2 (δ_C 171.7) suggested that one hydroxyl group was located at the oxygenated quaternary carbon C-6. The proton spin system of H-3 (δ_H 3.96)/H_2-4 (δ_H 2.06, 1.87)/H_2-5 (δ_H 2.50, 2.29) in the ^{1}H−^{1}H COSY spectrum (Figure S1, Supporting Information) and diagnostic correlations from H-7 (δ_H 2.37) to C-5 (δ_C 30.9) and H-3 (δ_H 3.96) to C-2 (δ_C 171.7) in the HMBC indicated that the remaining hydroxyl group was attached to C-3. The relative configuration of **5** was established as being similar to that of **3** via key ROESY correlations (Figure S2, Supporting Information). The β-orientation for H-3 was supported by the ROESY correlations of H-3 (δ_H 3.96)/H-10a (δ_H 4.42) and H-10a/H-9 (δ_H 2.63). The absolute configuration of **5**, (3*R*,6*S*,7*S*,9*S*), was elucidated via an ECD calculation (Figure 4).

Ormosianine F (**6**) had a molecular formula of $C_{16}H_{25}N_2O_3$ based on its HRESIMS (*m*/*z* 293.1863 [M + H]$^+$) data. The NMR data (Table 3) of **6** were almost the same as those of **3**, except for the observation of an additional methoxy group (δ_H 3.36, δ_C 48.5). The HMBC correlations (Figure 3) from OCH_3 (δ_H 3.36) to C-6 (δ_C 88.3) and from H_2-10 (δ_H 4.60, 2.88) to C-6 (δ_C 88.3)/C-2 (δ_C 171.6) confirmed that the methoxy was located at C-6. Conversely, the ROESY correlations (Figure S2, Supporting Information) of OCH_3-6 (δ_H 3.36)/H-7 (δ_H 2.14), H-8b (δ_H 1.81)/H-10a (δ_H 4.60), and OCH_3-6 (δ_H 3.36)/H-7 (δ_H 2.14) suggested the β-orientations for H-7, H-9, and OCH_3-6. The experimental ECD of compound **6** with one positive Cotton effect at 306 nm and two negative Cotton effects at 205 and 234 nm was in good agreement with that of calculated **3**. Accordingly, the absolute configuration of **6** was defined as (6*S*,7*S*,9*S*).

Ormosianine G (**7**) shared the same molecular formula of $C_{15}H_{22}N_2O_3$ as **3** based on the HRESIMS ion at *m*/*z* 277.1556 [M − H]$^-$ (calcd for $C_{15}H_{21}N_2O_3$, 277.1558). Its NMR

https://doi.org/10.1021/acs.jnatprod.3c00493
J. Nat. Prod. 2023, 86, 2193−2205

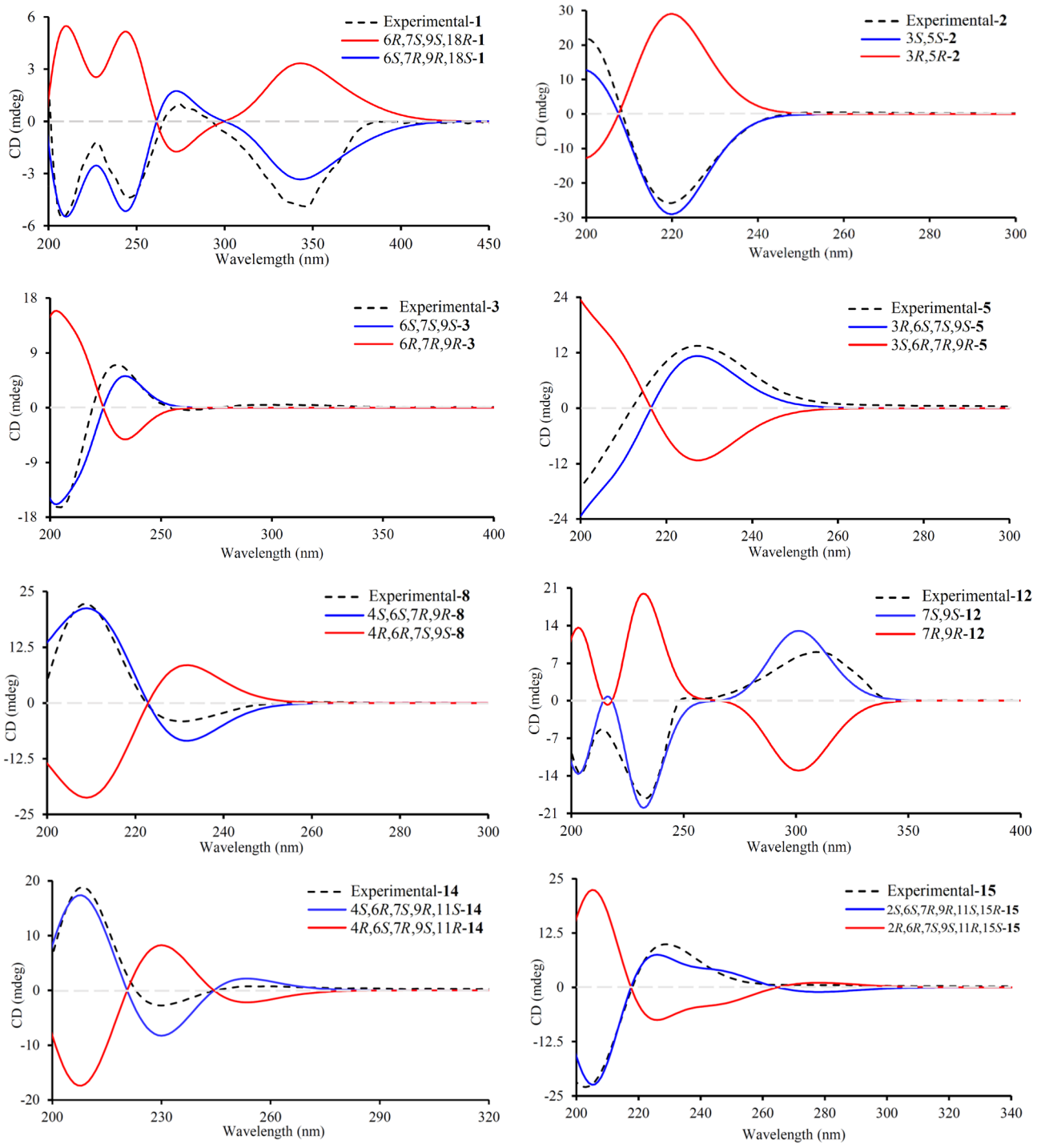

Figure 4. Experimental and calculated ECD spectra of **1**−**3**, **5**, **8**, **12**, **14**, and **15**.

spectroscopic spectra (Table 3) were similar to those of **3**, except for the presence of an oxygenated methine at δ_C 66.7 in **7**, instead of an oxygenated quaternary carbon at C-6 (δ_C 84.3) in the latter, indicating that the hydroxyl group was placed at the piperidine moiety. The placement of the hydroxyl group was proposed at C-5 based on the observed HMBC correlations (Figure S1, Supporting Information) from H-6 (δ_H 3.50) to C-5 (δ_C 66.7) and from H-5 (δ_H 4.32) to C-7 (δ_C 30.6), as well as by observing the proton spin system H-6 (δ_H 3.50)/H-5 (δ_H 4.32)/H_2-4 (δ_H 2.14, 1.87) in the $^1H-^1H$ COSY spectrum (Figure S1, Supporting Information). The relative configuration of **7** was assigned as being the same as that of **3** based on ROESY correlations (Figure S2, Supporting Information) of H-6/H-5, H-6/H-7 (δ_H 2.47), H-8b (δ_H 1.95)/H-7, and H-8b/H-9 (δ_H 2.64). The absolute configuration of **7** was established as (5*S*,6*S*,7*S*,9*S*) by ECD calculation (Figure S1, Supporting Information).

Ormosianines H−J (**8**−**10**) presented the same molecular formula of $C_{15}H_{22}N_2O_3$ as deduced from their HRESIMS ion peaks at *m*/*z* 301.1526 $[M + Na]^+$, 277.1559 $[M - H]^-$, and 279.1705 $[M + H]^+$, respectively. The NMR spectra (Table 4) of **8**−**10** closely resembled those of **7**, differing in the locations

https://doi.org/10.1021/acs.jnatprod.3c00493
J. Nat. Prod. 2023, 86, 2193−2205

Table 2. ^{13}C (125 MHz) and ^{1}H (500 MHz) NMR Data for 2 in $CDCl_3$

no.	δ_C, type	δ_H (mult., J in Hz)
2	172.4, C	
3	36.2, CH	2.84, dt (19.7, 1.6)
4	25.3, CH_2	2.12, t (3.2)
5	36.7, CH	2.82, dd (4.8, 3.1)
6	46.7, CH_2	3.54, m
		3.50, m
7	169.7, C	
8	117.1, CH_2	5.05, dq (17.1, 1.6)
		5.01, dt (10.2, 1.1)
9	134.8, CH	5.74, dt (17.2, 7.0)
10	31.5, CH_2	2.31, dd (8.3, 2.7)
		2.29, dd (7.1, 1.3)
11	45.9, CH_2	3.42, td (7.2, 1.8)
13	51.8, CH_2	3.54, m
		3.48, m

of the hydroxy groups. The hydroxyl groups were placed at C-4 (**8**), C-3 (**9**), and C-10 (**10**) by observing diagnostic HMBC correlations (Figure 5A and Figure S1, Supporting Information) from H-4 (δH 4.11) to C-2 (δ_C 168.5)/C-6 (δ_C 61.8), from H-3 (δ_H 3.91) to C-2 (δ_C 172.7), and from H-10 (δ_H 6.06) to C-2 (δ_C 172.5)/C-6 (δ_C 55.2)/C-11 (δ_C 168.8), respectively. In compound **8**, the ROESY correlations (Figure 5B) of H-4 (δ_H 4.11)/H-6 (δ_H 3.46) and H-6/H-7 (δ_H 3.28)/H-8a (δ_H 3.28) suggested the α-orientation of H-4. The correlations of H-7 to H-17b (δ_H 3.92) and H-10b (δ_H 2.64), as well as of H-6 to H-5b (δ_H 1.76) and H-8b (δ_H 2.35), established the methylene bridge (H-8) with α-orientation. For compound **9**, in the ROESY spectrum (Figure S2, Supporting Information), correlations of H-3 (δ_H 3.91)/H-6 (δ_H 3.48), H-6/H-7 (δ_H 1.98), and H-6/H-8a (δ_H 2.16) suggested that these protons were located at the cofacial side and with β-orientation. Likewise, the β-orientations of H-6, H-7, H-9, and H-10 in **10** were evidenced via ROESY correlations (Figure S2, Supporting Information) of H-6 (δ_H 3.87)/H-7 (δ_H 2.43), H-6/H-10 (δ_H 6.06), H-10/H-9 (δ_H 2.86), and H-7/H-9. Thanks to the ECD calculations (Figure 4 and Figure S3, Supporting Information), the absolute configurations of **8**–**10** were assigned as (4*S*,6*S*,7*R*,9*R*), (3*R*,6*R*,7*S*,9*S*), and (6*R*,7*S*,9*S*,10*S*), respectively.

Ormosianine K (**11**) had a molecular formula of $C_{15}H_{20}N_2O_2$ as defined by the HRESIMS molecular ion at m/z 261.1594 $[M + H]^+$ (calcd for $C_{15}H_{21}N_2O_2$, 261.1598). Inspection of the NMR data (Table 4) revealed that **11** presented an additional C-5/C-6 double bond in tetrahydro-11-oxorhombifoline (**17**).[19] This hypothesis was confirmed by the HMBC correlations (Figure S1, Supporting Information) from H-10 (δ_H 4.45) to C-2 (δ_C 170.1)/C-6 (δ_C 140.8) and from H-5 (δH 5.08) to C-7 (δ_C 33.4)/C-6 (δ_C 140.8) as well as the $^{1}H-^{1}H$ COSY correlations (Figure S1, Supporting Information) of H_2-3 (δ_H 2.47, 2.40)/H_2-4 (δ_H 2.28, 2.15) and H_2-4/H-5 (δ_H 5.08). The absolute configuration of **11** was established as (7*S*,9*S*) by comparison of its experimental ECD (Figure S1, Supporting Information) with the calculated analysis.

Ormosianine L (**12**) was obtained as a colorless oil. Its HRESIMS data displayed an ion peak at m/z 259.1440 $[M + H]^+$ (calcd for $C_{15}H_{19}N_2O_2$, 259.1441), suggesting a molecular formula of $C_{15}H_{18}N_2O_2$, with seven degrees of unsaturation. Analyses of the ^{1}H and ^{13}C NMR data (Table 4) revealed that compound **12** was structurally related to **11**, differing in that **12** presented an additional endocyclic double bond [δ_C 118.3 (d, C-3), δ_H 6.49 (1H, d, J = 9.1 Hz, H-3); δ_C 138.8 (d, C-4), δ_H 7.29 (1H, dd, J = 9.1, 6.9 Hz, H-4)]. This assumption was supported by key HMBC correlations (Figure 3) from H_2-10 (δ_H 4.53, 3.72) to C-2 (δ_C 163.1)/C-6 (δ_C 148.6) and from H-4 (δ_H 7.29) to C-2, as well as $^{1}H-^{1}H$ COSY cross-peaks (Figure 3) of H-5 (δ_H 6.08)/H-4 (δ_H 7.29)/H-3 (δ_H 6.49). The absolute configuration of **12** (7*S*,9*S*) was established by ECD calculations (Figure 4).

Ormosianine M (**13**) was isolated as a colorless oil and found to possess the molecular formula $C_{17}H_{26}N_2O_4$, as defined by the HRESIMS molecular ion at m/z 323.1969 $[M + H]^+$ (calcd for $C_{17}H_{27}N_2O_4$, 323.1965). Examination of ^{1}H and ^{13}C NMR spectra (Table 5) indicated that compound **13** is an analogue of sparteine (tetracyclic type), bearing the characteristic signals as two nitrided methine signals [δ_C 61.4 (C-6), δ_H 3.30 (H-6); δ_C 57.8 (C-11), δ_H 2.10 (H-11)] and two common methines shared by a bis-quinolizidine unit [δ_C 32.2 (C-7), δ_H 1.97 (H-7); δ_C 33.7 (C-9), δ_H 1.54 (H-9)]. The above NMR data suggested **13** was a derivative of 13-epihydroxylupanine acetate (**23**)[20] bearing an extra hydroxyl group at C-3. This hypothesis was confirmed by observation of HMBC correlations (Figure 3) from H-6 (δ_H 3.30) to C-2 (δ_C 173.6) and from H-3 (δ_H 3.98) to C-2 (δ_C 173.6), as well as by the presence of a proton spin system including H-3 (δ_H 3.98)/H_2-4 (δ_H 2.16, 1.62)/H_2-5 (δ_H 1.76, 1.61)/H-6 (δ_H 3.30) in the $^{1}H-^{1}H$ COSY spectrum (Figure 3). The ROESY cross-peaks (Figure S2, Supporting Information) of H-3 (δ_H 3.98)/H-6 (δ_H 3.30)/Ha-8 (δ_H 2.09) indicated the α-orientation for OH-3. The absolute configuration of **13** was elucidated as 3*R*,6*R*,7*S*,9*S*,11*S*,13*S* by ECD calculations (Figure S3, Supporting Information).

Ormosianine N (**14**) was obtained as a colorless oil. Its molecular formula was assigned as $C_{15}H_{24}N_2O_2$ by the HRESIMS ion at m/z 265.1911 $[M + H]^+$ (calcd for $C_{15}H_{25}N_2O_2$, 265.1911). The NMR data (Table 5) suggested that **14** shared the same scaffold as that of **13** with the absence of a C-4 side chain. The presence of a hydroxyl group at C-4 and a carbonyl group at C-10 was evident from the key HMBC correlations (Figure 3) from H-6 (δ_H 3.33)/H_2-2 (δ_H 4.81, 2.45) to C-10 (δ_C 172.5)/C-4 (δ_C 69.3). Both H-4 and H-6 were β-oriented, as deduced from the ROESY cross-peaks (Chart S2, Supporting Information) of H-4 (δ_H 3.79)/H-8a (δ_H 1.91) and H-4/H-6 (δ_H 3.33). The absolute configuration of **14** was assigned as (4*S*,6*R*,7*S*,9*R*,11*S*) by ECD calculations (Figure 4).

Ormosianine O (**15**) presented the molecular formula of $C_{15}H_{24}N_2O_2$ with 16 mass units more than that of **14** by an HRESIMS ion at m/z 281.1859 $[M + H]^+$ (calcd for $C_{15}H_{25}N_2O_3$, 281.1860). Analyses of the NMR data (Table 5) revealed that **14** and **15** shared the same skeleton (sparteine) type. The HMBC correlations (Figure 3) from H-6 (δ_H 3.84) to C-2 (δ_C 69.6)/C-10 (δ_C 54.9) and from H_2-15 (δ_H 4.77, 2.70) to C-11 (δ_C 63.0)/C-14 (δ_C 171.0)/C-17 (δ_C 55.6) indicated that one carbonyl and two hydroxyl groups were placed at C-14, C-2, and C-15, respectively. The ROESY correlations (Figure S2, Supporting Information) of H-8a (δ_H 2.25)/H-6 (δ_H 3.84), H-7 (δ_H 1.65)/H-9 (δ_H 1.81), H-7 (δ_H 1.65)/H-6 (δ_H 3.84), H-2 (δ_H 3.57)/H-17a (δ_H 3.03), and H-9 (δ_H 1.81)/H-11 (δ_H 2.04) revealed that these hydrogens were α-oriented. In contrast, the ROESY correlations of H-15b (δ_H

https://doi.org/10.1021/acs.jnatprod.3c00493
J. Nat. Prod. 2023, 86, 2193−2205

Table 3. ^{13}C (125 MHz) and ^{1}H (500 MHz) NMR Data for 3−7

	3[a]		4[b]		5[a]		6[a]		7[a]	
no.	δ_C, type	δ_H (mult., J in Hz)	δ_C, type	δ_H (mult., J in Hz)	δ_C, type	δ_H (mult., J in Hz)	δ_C, type	δ_H (mult., J in Hz)	δ_C, type	δ_H (mult., J in Hz)
2	171.1, C		169.6, C		171.7, C		171.6, C		169.8, C	
3	33.2, CH_2	2.42, m	30.9, CH_2	2.15, overlap	67.3, CH	3.96, dd (11.9, 4.1)	32.8, CH_2	2.36, q (6.5)	27.8, CH_2	2.61, t (8.0)
		2.21, m		2.13, m						2.34, t (8.1)
4	34.1, CH_2	2.08, overlap	24.0, CH_2	1.99, qd (11.6, 7.7)	23.4, CH_2	2.06, m	18.4, CH_2	1.95, m	30.3, CH_2	2.14, dt (13.0, 3.5)
		1.83, d (10.4, 2.4)		1.64, dq (11.8, 3.1)		1.87, dd (12.6, 4.0)		1.65, m		1.87, overlap
5	16.1, CH_2	2.07, m	66.6, CH	3.89, dd (11.3, 4.0)	30.9, CH_2	2.50, td (12.2, 5.5)	29.5, CH_2	2.05, m	66.7, CH	4.32, td (6.1, 3.1)
		1.72, td (8.8, 6.3)				2.29, m		1.95, m		
6	84.3, C		84.8, C		85.3, C		88.3, C		62.6, CH	3.50, dd (8.0, 2.2)
7	38.0, CH	2.11, m	32.6, CH	2.32, d (14.5)	33.5, CH	2.37, overlap	37.2, CH	2.14, brs	30.6, CH	2.47, brs
8	23.5, CH_2	1.85, brs	23.2, CH_2	2.25, m	24.1, CH_2	2.37, m	24.0, CH_2	2.45, dq (12.7, 3.1)	28.7, CH_2	1.85, m
		1.84, td (10.4, 4.6)		1.77, m		1.86, m		1.81, dq (12.7,3.1)		1.95, m
9	37.6, CH	2.60, brs	36.8, CH	2.43, brs	37.3, CH	2.63, dq (5.3, 2.7)	37.3, CH	2.59, brs	37.7, CH	2.64, overlap
10	41.3, CH_2	4.45, dt (13.2, 2.0)	41.6, CH_2	4.11, dt (12.8, 2.2)	42.4, CH_2	4.42, dt (13.2, 2.3)	41.3, CH_2	4.60, dt (13.1, 2.1)	46.4, CH_2	4.86, dt (13.3, 2.2)
		3.09, m		2.93, dd (12.9, 3.3)		3.12, m		2.88 dd (13.1, 3.2)		2.72, dd (13.3, 3.3)
11	170.9, C		170.0, C		171.5, C		170.4, C		170.3, C	
12	116.8, CH_2	5.03, dq (17.0, 1.6)	116.3, CH_2	5.04, m	117.1, CH_2	5.05, dt (17.2, 1.7)	116.8, CH_2	5.05, dt (17.1, 1.6)	116.6, CH_2	5.05, dd (16.0, 4.1)
13		4.99, dq (10.2, 1.4)		4.97, dd (10.1, 2.0)		5.04, dq (10.2, 1.3)		5.00, dd (10.3, 1.6)		5.00, dd (16.0, 4.1)
	135.0, CH	5.70, dt (17.0, 6.8)	135.8, CH	5.70, dt (17.0, 6.7)	135.2, CH	5.74, dt (16.9, 6.8)	135.1, CH	5.73, dt (17.1, 6.8)	135.4, CH	5.74, dt (17.0, 6.7)
14	31.4, CH_2	5.03, dq (17.0, 1.6)	30.8, CH_2	2.15, m	31.6, CH_2	5.09, dt (17.2, 1.7)	31.4, CH_2	5.05, dt (17.1, 1.6)	31.3, CH_2	2.26, m
		2.21, m		2.15, m		2.29, m		2.25, m		2.26, m
15	45.7, CH_2	2.21, m	44.6, CH_2	2.15, m	46.1, CH_2	2.28, m	45.9, CH_2	2.25, m	45.9, CH_2	2.26, m
		3.59, dd (13.6, 6.5)		2.15, m		3.63, m		3.47, d (8.2)		2.26, m
17	48.8, CH_2	3.10, dt (5.4, 1.4)	47.6, CH_2	3.32, dd (3.4, 5.0)	48.6, CH_2	3.12, overlap	48.5, CH_2	3.27 m	49.0, CH_2	4.11, dt (13.1, 1.3)
		3.40, brs		3.32, dd (3.4, 5.0)		3.39, m		3.44, m		
OCH_3							48.5, CH_3	3.36, brs		

[a]Measured in $CDCl_3$. [b]Measured in DMSO-d_6.

https://doi.org/10.1021/acs.jnatprod.3c00493
J. Nat. Prod. 2023, 86, 2193−2205

Table 4. ^{13}C (125 MHz) and ^{1}H (500 MHz) NMR Data of 8−12

	8[a]		9[b]		10[b]		11[b]		12[b]	
no.	δ_C, type	δ_H (mult., J in Hz)	δ_C, type	δ_H (mult., J in Hz)	δ_C, type	δ_H (mult., J in Hz)	δ_C, type	δ_H (mult., J in Hz)	δ_C, type	δ_H (mult., J in Hz)
2	168.5, C		172.7, C		172.7, C		170.1, C		163.1, C	
3	27.9, CH_2	2.36, brs	68.0, CH	3.91, dd (12.1, 5.6)	27.6, CH_2	1.80, overlap	31.4, CH_2	2.47, dd (5.9, 1.2)	118.3, CH	6.49, d (9.1)
		1.76, dd (14.0, 7.8)				1.75, overlap		2.40, td (15.0, 1.0)		
4	65.1, CH	4.11, brs	27.5, CH_2	2.30 m	32.3, CH_2	2.29, m	19.3, CH_2	2.28, overlap	138.8, CH	7.29, dd (9.1, 6.9)
				1.69, qd (12.2, 4.8)		2.00, tt (5.5, 2.6)		2.15, dd (6.2, 3.0)		
5	28.0, CH_2	2.08, d (6.0)	24.5, CH_2	1.88, m	20.1, CH_2	1.92, m	105.0, CH	5.08, dd (6.4, 2.9)	105.7, CH	6.08, d (6.9)
		1.76, dd (14.0, 7.8)				1.74, overlap				
6	61.8, CH	3.46, overlap	60.5, CH	3.48, m	55.2, CH	3.87, m	140.8, C		148.6, C	
7	29.5, CH	3.28, brs	32.4, CH	1.98, brs	33.2, CH	2.43, overlap	33.4, CH	2.82, dq (8.4, 2.0)	33.4, CH	3.28, brs
8	29.6, CH_2	2.35, overlap	28.9, CH_2	2.16, dq (12.0, 4.3)	22.7, CH_2	2.40, m	26.1, CH_2	2.05, dt (12.8, 2.1)	23.6, CH_2	2.20, m
		2.08, d (6.0)		1.87, m		1.93, m		1.91, dt (12.8, 2.0).		2.07, dt (13.1, 2.2)
9	37.4, CH	2.39, brs	37.3, CH	2.69, brs	43.2, CH	2.86, m	36.8, CH	2.82, dq (8.4, 2.0)	36.4, CH	3.13, overlap
10	45.4, CH_2	4.51, dt (12.9, 2.1)	46.3, CH_2	4.65, dt (13.4, 2.2)	73.9, CH	6.06, d (2.7)	45.8, CH_2	4.45, dt (13.3, 2.0)	48.6, CH_2	4.53, d (15.2)
		2.64, dd (12.8, 3.1)		2.81 dd (13.6, 3.2)				3.60, m		3.72, td (15.2, 5.5)
11	169.5, C		170.0, C		168.8, C		169.7, C		169.2, C	
12	116.2, CH_2	5.01, dd, (17.2, 2.0)	116.9, CH_2	5.01, m	116.8, CH_2	5.05, m	116.8, CH_2	5.01, m	117.0, CH_2	4.90, m
13		4.95, dd (10.2, 2.1)		5.01, m		5.01, m		4.98, m		4.75, m
	135.8, CH	5.60, dt (17.1, 6.7)	135.1, CH	5.72, dt (17.1, 6.7)	135.2, CH	5.74, dt (17.0, 6.8)	135.1, CH	5.70, dt, J = 17.1, 6.9)	134.6, CH	5.60, dt (17.1, 7.0)
14	30.9, CH_2	5.01, dd, (17.2, 2.0)	31.4, CH_2	2.25, m	31.5, CH_2	2.29, m	31.5, CH_2	2.27, m	31.5, CH_2	2.20, m
		2.11, m		2.25, m		2.27, m		2.27, m		2.20, m
15	44.8, CH_2	2.11, m	45.8, CH_2	2.25, m	45.9, CH_2	2.29, m	45.6, CH_2	2.27, m	45.4, CH_2	2.20, m
		3.42, overlap		2.25, m		2.27, m		2.27, m		2.20, m
17	48.3, CH_2	3.29, m	46.7, CH_2	3.40, d (13.1)	46.5, CH_2	3.42, brs	56.1, CH_2	3.58, m	56.1, CH_2	3.70, td (9.1, 5.5)
		3.92, d (12.9)		3.34, dd (13.1, 6.0),		3.31, dd (13.0, 5.9)		3.20, dt (11.9, 1.7)		3.30, m

[a]Measured in DMSO-d_6. [b]Measured in $CDCl_3$.

https://doi.org/10.1021/acs.jnatprod.3c00493
J. Nat. Prod. 2023, 86, 2193−2205

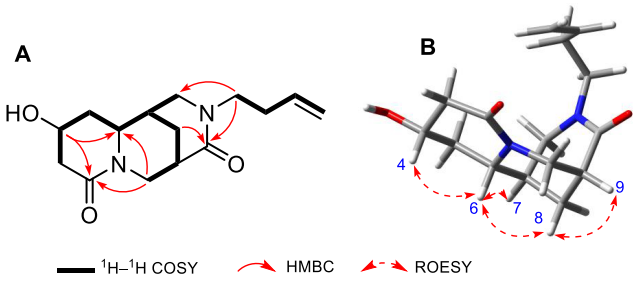

Figure 5. Key (A) ^{1}H–^{1}H COSY, HMBC, and (B) ROESY correlations of **8**.

2.70)/H-17b (δ_H 2.16) indicated that H-15 was β-oriented. The absolute configuration of **15** was finally elucidated as (2*S*,6*S*,7*R*,9*R*,11*S*,15*R*) based on analyses of its experimental and calculated ECD data (Figure 4).

Ormosianine P (**16**) presented the molecular formula $C_{22}H_{37}N_3O$ at *m*/*z* 360.2975 [M + H]$^+$ (calcd for $C_{23}H_{38}N_3O$, 360.3009) in the HRESIMS spectrum. The ^{13}C NMR spectrum (Table 6) revealed 22 carbon signals corresponding to one amide-carbonyl group [C-24 (δ_C 179.8)], one quaternary carbon [C-9 (δ_C 39.9)], three methine groups [C-6 (δ_C 63.8), C-11 (δ_C 66.5), and C-18 (δ_C 66.2)], along with 13 methylenes including four nitrogenated methylenes [C-2 (δ_C 55.6), C-10 (δ_C 55.6), C-13 (δ_C 46.6), and C-22 (δ_C 47.7)]. Detailed interpretation of the NMR data (Table 6) indicated that compound **16** has the same parent skeleton as that of piptanthin (**26**),[21] except for the presence of an additional acetyl group [CH_3-25 (δ_H 1.90), C-25 (δ_C 22.8); C-24 (δ_C 179.8)]. The key HMBC correlations (Figure 6) from H-18 (δ_H 2.67)/CH_3-25 (δ_H 1.90) to C-24 (δ_C 179.8) established that the acetyl group was located at N-23. The ROESY correlations (Figure 6) of H-8a (δ_H 1.66)/H-6 (δ_H 2.40)/H-10b (δ_H 2.59) and H-8b (δ_H 1.27)/H-11(δ_H 2.78)/H-18 (δ_H 2.67) revealed that these hydrogens were α-oriented, whereas the observed ROESY correlations of H-16 (δ_H 2.47)/H-17a (δ_H 1.63)/H-10a (δ_H 2.93) revealed that these hydrogens were β-oriented. The absolute configuration of **16** was established as (6*R*,7*R*,9*R*,11*S*,16*R*,18*S*) by ECD calculations (Figure S3, Supporting Information).

In addition, 18 known constituents, named tetrahydro-11-oxorhombifoline (**17**),[19] oxoaphyllidine (**18**),[22] hydroxylupanine (**19**),[23] pseudohydroxylupanine (**20**),[24] 13-methoxylupanine (**21**),[25] oxylupanine acetate (**22**),[26] 13-epihydroxylupanine acetate (**23**),[27] homopodopetaline (**24**),[17] 6-epihomopodopetaline (**25**),[18] piptanthin (**26**),[21] ormocastrine (**27**),[28] *N*′-acetylormosanine (**28**),[29] ormosanine (**29**),[30] homoormosanine (**30**),[31] homopiptanthine (**31**),[21] 9-β-D-ribofuranosyladenine (**32**),[32] *N*-(hydroxymethyl)adenosine (**33**),[33] and uridine (**34**),[34] were identified by comparison of their spectroscopic data with literature data.

Acetylcholinesterase (AChE) inhibitors are a group of drugs that block the normal breakdown of acetylcholine, which are divided as irreversible and reversible.[35] Reversible AChE inhibitors can be used for the treatment of human neurodegenerative disorders including Alzheimer's disease, such as donepezil, rivastigmine, and galantamine.[36] Also, toxic organo-

Table 5. ^{13}C (125 MHz) and ^{1}H (500 MHz) NMR Data for 13−15 in $CDCl_3$

	13		14		15	
no.	δ_C, type	δ_H (mult., *J* in Hz)	δ_C, type	δ_H (mult., *J* in Hz)	δ_C, type	δ_H (mult., *J* in Hz)
2	173.6, C		40.2, CH_2	4.81, dt (13.4, 2.6)	69.6, CH	3.57, d (11.9)
				2.45, td (13.4, 2.6)		
3	68.1, CH	3.98, m	34.3, CH_2	1.91, m	40.1, CH_2	1.74, m
				1.46, td (13.1, 7.3)		1.57, overlap
4	27.3, CH_2	2.16, m	69.3, CH	3.79, dt (15.0, 4.2)	35.3, CH_2	1.84, m
		1.62, td (11.2, 2.4)				1.39, brs
5	24.5, CH_2	1.76, m	37.9, CH_2	1.83, m	24.3, CH_2	1.86, m
		1.61, dt (15.4, 2.1)		1.60, m		
6	61.4, CH	3.30, td (10.8, 1.8)	56.9, CH	3.33, brs	68.4, CH	3.84, brs
7	32.2, CH	1.97, m	32.3, CH	1.99, m	33.8, CH	1.65, overlap
8	26.1, CH_2	2.09, m	23.2, CH_2	1.91, m	27.2, CH_2	2.25, dd (10.4, 2.2)
		1.24, dt (12.5, 2.6)		1.63, m		1.67, overlap
9	33.7, CH	1.54, m	43.9, CH	2.35, brs	33.9, CH	1.81, m
10	47.8, CH_3	4.25, dt (13.4, 2.3)	172.5, C		54.9, CH_2	2.65, dd (13.2, 5.8)
		2.63, td (13.4, 2.3)				1.78, overlap
11	57.8, CH	2.10, m	58.9, CH	3.05, m	63.0, CH	2.04, d (6.4)
12	35.9, CH_2	1.63, m	22.5, CH_2	1.85, m	34.7, CH_2	1.81, m
				1.15, m		1.38, td (15.1, 4.6)
13	68.1, CH	4.98, sept (2.9)	25.6, CH_2	1.83, m	59.2, CH	3.56, d (11.9)
				1.46, td (17.4, 2.6)		
14	28.4, CH_2	1.77, m	18.9, CH_2	1.60, m	171.0, C	
		1.63, td (11.2, 2.4)		1.12, m		
15	49.4, CH_2	2.53, m	54.2, CH_2	2.73, m	43.1, CH_2	4.77, d (13.9)
		2.29, m		2.66, overlap		2.70, dd (13.2, 2.2)
17	51.6, CH_2	2.86, dd (11.7, 9.3)	46.7, CH_2	3.08, m	55.6, CH_2	3.03, d (11.9)
		2.04, overlap		2.57 d (11.6)		2.16, d (11.9)
18	170.6, C					
19	21.5, CH_3	2.02, s				

https://doi.org/10.1021/acs.jnatprod.3c00493
J. Nat. Prod. 2023, 86, 2193−2205

Table 6. ^{13}C (125 MHz) and ^{1}H (500 MHz) NMR Data of 16 in CD_3OD

no.	δ_C, type	δ_H (J in Hz)	no.	δ_C, type	δ_H (J in Hz)
2	55.6, CH_2	2.82, d (12.4)	14	25.5, CH_2	1.78, m
		2.74, brs			1.68, brs
3	26.3, CH_2	1.66, m	15	32.8, CH_2	1.77, m
		1.37, dd (14.3, 5.6)			1.20, m
4	23.9, CH_2	1.89, brs	16	35.3, CH	2.47, d (11.9)
		1.89, brs	17	38.6, CH_2	1.63, m
5	29.6, CH_2	1.58, m			1.19, m
		1.31, d (12.8)	18	66.2, CH	2.67, m
6	63.8, CH	2.40, d (11.6)	19	26.3, CH_2	1.88, overlap
7	35.7, CH	1.68, m			1.77, m
8	30.8, CH_2	1.66, m	20	25.1, CH_2	1.88, overlap
		1.27, d (7.8)			1.67, brs
9	39.9, C		21	25.9, CH_2	1.45, dt (17.1, 4.0)
10	55.6, CH_2	2.93, d (13.0)			3.17, d (12.2)
		2.59, dt (12.5, 2.7)	22	47.7, CH_2	1.37, dd (14.3, 3.6)
11	66.5, CH	2.78, d (10.8)			2.60, td (12.5, 2.7)
13	46.6, CH_2	3.27, dd (12.8, 4.4)	24	179.8, C	
		2.88, dd (13.0, 3.2)	25	22.8, CH_3	1.90, s

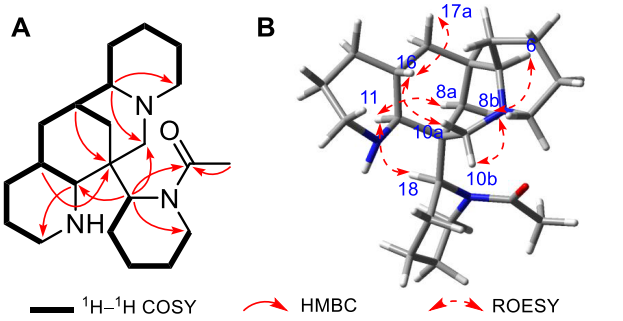

Figure 6. Key (A) ^1H–^1H COSY, HMBC, and (B) ROESY correlations of **16**.

Table 7. Acetylcholinesterase Inhibitory Effects of 1, 4, 6, 11–13, 16, 24, and 27–29

	AChE		AChE
compound	IC_{50} ± SD (μM)[a]	compound	IC_{50} ± SD (μM)[a]
1	1.55 ± 0.14	**24**	5.23 ± 1.10
4	29.60 ± 3.17	**27**	16.97 ± 0.68
6	15.71 ± 0.96	**28**	8.48 ± 0.64
11	20.02 ± 2.32	**29**	5.56 ± 1.12
12	12.84 ± 1.04	huperzine A	0.12 ± 0.04
13	9.77 ± 2.11	chlorpyrifos	23.33 ± 1.43 (nM)
16	5.65 ± 0.79		

[a]All experiments were performed in triplicate.

phosphorus and carbamate insecticides act as AChE inhibitors and can be used as pesticides in agriculture.[37] However, agricultural workers would suffer from the underlying risk of poisoning if they are exposed to high concentrations of these organophosphorus pesticides in the long term. It is estimated that hundreds of thousands people, especially those living in rural areas of developing countries, are poisoned by organophosphorus pesticides every year.[38] Thus, the search for more AChE inhibitors from natural plants is important for the development of low-toxicity, effective insecticides. Based on the fact that QAs are poisonous to insects, alkaloids obtained from *O. yunnanensis* were evaluated for their insect AChE inhibitory effects. As indicated in Table 7 (Figure S2, Supporting Information), 11 compounds (**1**, **4**, **6**, **11**–**13**, **16**, **24**, and **27**–**29**) displayed AChE inhibitory activities with IC_{50} values ranging from 1.55 to 29.60 μM. Among them, compound **1** displayed the most potent AChE inhibitory activity, with an IC_{50} value of 1.55 ± 0.14 μM. Taken together, *Ormosia*-type QAs with the pentacycline system, including **1**, **16**, **24**, and **27**–**29**, presented better AChE inhibition effects.

In light of the observed AChE inhibitory activities (Table 7), the most active QA, **1**, and three different types of active compounds, including **12**, **13**, and **16**, along with the positive controls (huperzine A (Hup A) and chlorpyrifos (CPF)), were selected to perform molecular docking studies to clarify their potential mechanism of action as acetylcholinesterase inhibitors (PDB ID: 1DX4) (Figure 7). The positive controls CPF and Hup A could bind to AChE with energies of −7.2 and −9.3 kcal/mol, respectively. The phosphoric acid group of the former formed strong hydrogen bonds with THR-154 and TYR-370 residues of 1DX4 (Figure 7A), whereas the exocyclic amino group of the latter formed only one hydrogen bond with the residue TYR-370 (Figure 7B). Compound **1** could interact with AChE with a binding energy of −8.8 kcal/mol, forming three hydrogen bonds with SER-238 and HIS-480 (Figure 7C). The binding energy of **12** to AChE is −9.4 kcal/mol, and it formed two hydrogen bonds with SER-238 and THR154 (Figure 7D). **13** could form two hydrogen bonds with GLY-151 and TRP-83 residues of AChE (Figure 7E) with the binding energy of −7.5 kcal/mol. For compound **16**, a strong hydrogen bond interaction with the THR-154 residue with a binding energy of −8.2 kcal/mol was measured (Figure 7F). Although more negative values are always associated with higher affinity and possible higher inhibition, there appears to be no significant correlation between the stabilization of the complex and the IC_{50} inhibition values for the molecular docking studies. The energy data for compounds **1** (−8.8 kcal/mol), **12** (−9.4 kcal/mol), **13** (−7.5 kcal/mol), and **16** (−8.2 kcal/mol) are more negative than the reference (chlopyrifos, −7.2 kcal/mol), indicating that compounds **1**, **12**, **13**, and **16** are more potent AChE inhibitors than the control.

In summary, investigation of the stems and leaves of *O. yunnanensis* led to the isolation of 16 new quinolizidine alkaloids (ormosianines A–P) and 18 known analogs.

https://doi.org/10.1021/acs.jnatprod.3c00493
J. Nat. Prod. 2023, 86, 2193−2205

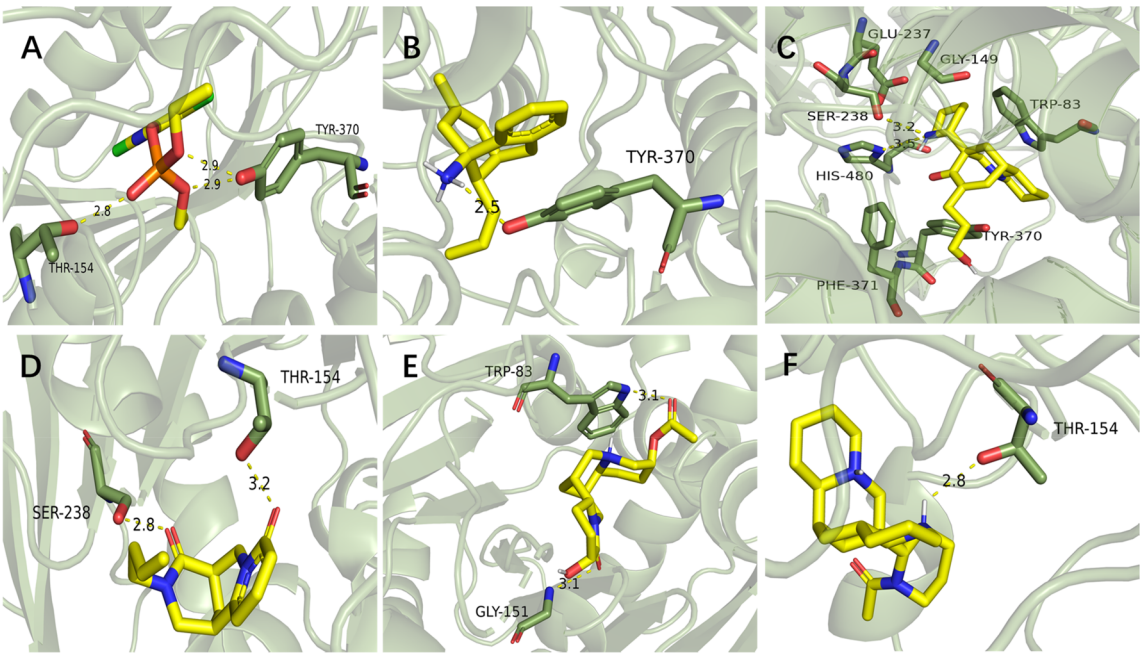

Figure 7. Molecular docking simulations of the binding poses of compounds **1**, **12**, **13**, **16**, CPF, and Hup A with 1DX4.

Ormosianine A (**1**), the first example of an *Ormosia*-type alkaloid with the cleaved piperidine ring, exhibited the most potent AChE inhibitory activity with an IC_{50} value of 1.55 μM. Molecular docking revealed the formation of hydrogen bonds between **1** and SER-238 and HIS-480 in the protein 1DX4. Our results enriched the structural diversity of QAs from the plants of the *Ormosia* genus and presented potent natural AChE inhibitors for further investigation.

EXPERIMENTAL SECTION

General Experimental Procedures. Optical rotations were determined on a JASCO DIP-1020 automatic digital polarimeter. UV and ECD spectra were taken on the Shimadzu UV-2401-PC spectrometer, using a MOS 450 detector (Bio-Logic Science Instruments, Seyssinet-Pariset, France). IR spectra were recorded on a Bruker Tensor-27 FT-IR infrared spectrometer using KBr pellets. 1D and 2D NMR spectra were carried out using Bruker AVANCE III-500 or AV-600 MHz NMR spectrometers with tetramethylsilane (TMS) as an internal standard, and chemical shifts were given as δ (ppm). The residual solvent peaks were given as $CDCl_3$ (δ_H 7.26, δ_C 77.1), DMSO-d_6 (δ_H 2.50, δ_C 39.6), and CD_3OD (δ_H 3.31, δ_C 48.8). HRESIMS data were obtained on an Agilent 1290 UPLC/6540 Q-TOF mass spectrometer. Column chromatography (CC) was performed on silica gel (100−200 and 200−300 mesh, Qingdao Marine Chemical Co. Ltd., P.R. China), Sephadex LH-20 (Pharmacia Fine Chemicals, Uppsala, Sweden), and C18 reversed-phase (Rp 18) silica gel (150−200 mesh, Merck, Germany). Semipreparative HPLC was performed on a Waters 600 binary pump system with a Waters 2489 detector (210 and 230 nm) using a YMC-Pack ODS-A column (250 × 10 mm, S-5 μm, 12 nm, Tokyo, Japan) or an X-Bridge Prep-C_{18} HPLC column (10 × 250 mm, 5 μm, Waters, Ireland). The other experimental procedures were carried out as previously described.[39,40]

Plant Material. Stems and leaves of *O. yunnanensis* were collected in Xishuangbanna Dai Autonomous Prefecture, south of Yunnan Province, China. It was identified by Prof. Chun-Fen Xiao (Xishuangbanna Tropical Botanical Garden, CAS). A voucher specimen (No. Luo20211001) was deposited at the Kunming Institute of Botany, CAS.

Extraction and Isolation. Air-dried bark and leaves of *O. yunnanensis* (8.0 kg) was powdered and extracted with MeOH (3 × 20 L). The residue (850 g) was subsequently dissolved with 0.1% (v/v) aqueous hydrochloric acid adjusting the pH to 2−3. The filtered solution was subsequently alkalized to pH 9−10 with 10% (v/v) ammonia and extracted with EtOAc (5 L × 4) to obtain the total alkaloid fraction (40 g). This fraction was separated by silica gel CC eluted with $CHCl_3$/MeOH (30:1 → 0:1, v/v) to provide four fractions (Fr. A−Fr. D). Fr. A (1.0 g) was further separated by silica gel CC (petroleum ether/acetone, 9:1 → 0:1, v/v) to obtain compounds **2** (20.0 mg) and **7** (13 mg). Fr. B (12.0 g) was separated by a silica gel CC (petroleum ether/acetone, 5:1 → 0:1, v/v) to yield four subfractions (Fr. B_1−Fr. B_4). Fr. B_1 (3.0 g) was purified by an MPLC-Rp-18 column (MeOH/H_2O, 60% → 100%, v/v) to afford compounds **3** (8.0 mg), **6** (29 mg), **11** (17 mg), **14** (4.0 mg), and **24** (40 mg). Similarly, Fr. B_2 (2.0 g) was further separated by an MPLC-Rp-18 column (MeOH/H_2O, 85%) to give compound **9** (70.0 mg). Compounds **5** (16 mg), **8** (5.0 mg), and **17** (2.3 g) were obtained from Fr. B_3 (5.0 g), separated by silica gel CC (petroleum ether/acetone, 5:1 → 0:1, v/v), and further purified by CC on a Sephadex LH-20 (MeOH) column. Fr. B_4 (2.0 g) was separated by semipreparative HPLC (MeOH/H_2O, 40% → 80%, v/v, 3.0 mL/min) to yield **1** (6.0 mg), **4** (50 mg), **12** (16 mg), **15** (23 mg), **22** (12 mg), and **16** (8.0 mg). Fr. C (12.0 g) was separated by reversed-phase MPLC with a C18 column (MeOH/H_2O, 40% → 100%, v/v) to yield three subfractions (Fr. C_1−Fr. C_3). Fr. C_1 (2.0 g) was purified by silica gel CC ($CHCl_3$/MeOH, 9:1 → 0:1, v/v) to give compounds **23** (3.0 mg) and **25** (1.1 g). Fr. C_2 (2.0 g) was subjected to a separation by CC on a C18 column (MeOH/H_2O, 20% → 100%, v/v), to afford compounds **10** (12 mg), **13** (7.0 mg), **19** (14 mg), **27** (11.0 mg), **29** (10 mg), and **34** (4.0 mg). Fr. C_3 (3.0 g) was separated by CC on Sephadex LH-20 (MeOH) and further purified by semipreparative HPLC (MeCN/H_2O, 10% → 60% v/v, 3.0 mL/min) to afford **18** (6.0 mg), **20** (10 mg), **21** (5.0 mg), **24** (7.0 mg), and **30** (25 mg). Fr. D (11.0 g) was subjected to reserved-phase MPLC on a C18 column (MeOH/H_2O, 3:7 → 1:0, v/v), to give three fractions (Fr. D_1 to D_3). Compounds **19** (3.0 mg), **26** (50 mg), **28** (6.0 mg), **31** (15 mg), and **33** (16 mg) were purified by preparative HPLC (MeOH/H_2O, 10% → 50%, v/v) from Fr. D_1 (5.0 g). Fr. D_2 (2.0 g) was chromatographed on silica gel CC ($CHCl_3$/MeOH, 4:1, v/v) to yield compounds **27** (17 mg) and **32** (40 mg).

*Ormosianine A (**1**):* white powder; $[\alpha]_D^{20}$ −23.2 (*c* 0.12, CH_3OH); UV (CH_3OH) λ_{max} (log ε) 245 (2.35), 222 (2.19), 198 (2.61) nm; IR (KBr) ν_{max} 3434, 2932, 1637, 1445, 1382, 1054 cm^{-1}; ECD (CH_3OH) λ_{max} ($\Delta\varepsilon$) 346 (+0.34), 276 (+0.06), 246 (−0.30), 229

https://doi.org/10.1021/acs.jnatprod.3c00493
J. Nat. Prod. 2023, 86, 2193−2205

(−0.10), 209 (−0.38), 192 (+0.91) nm; ^{1}H and ^{13}C NMR data, see Table 1; HRESIMS *m/z* 333.2537 [M + H]$^+$ (calcd for $C_{20}H_{33}N_2O_2$, 333.2573).

Ormosianine B (**2**): colorless oil; $[\alpha]_D^{21}$ −76.9 (*c* 0.13, CH_3OH); UV (CH_3OH) λ_{max} (log ε) 204 (3.97) nm; IR (KBr) ν_{max} 3434, 2936, 1639, 1496, 1361 cm^{-1}; ECD (CH_3OH) λ_{max} ($\Delta\varepsilon$) 219 (−14.78), 200 (+12.37) nm; ^{1}H and ^{13}C NMR data, see Table 2; HRESIMS *m/z* 209.1282 [M + H]$^+$ (calcd for $C_{11}H_{17}N_2O_2$, 209.1285).

Ormosianine C (**3**): colorless oil; $[\alpha]_D^{22}$ −24.8 (*c* 0.11, CH_3OH); UV (CH_3OH) λ_{max} (log ε) 204 (4.24) nm; IR (KBr) ν_{max} 3432, 2936, 1636, 1362, 1174 cm^{-1}; ECD (CH_3OH) λ_{max} ($\Delta\varepsilon$) 300 (+0.28), 263 (−0.24), 233 (+3.84), 204 (−9.50) nm; ^{1}H and ^{13}C NMR data, see Table 3; HRESIMS *m/z* 297.1688 [M + H]$^+$ (calcd for $C_{15}H_{23}N_2O_3$, 297.1703).

Ormosianine D (**4**): colorless oil; $[\alpha]_D^{19}$ −72.6 (*c* 0.07, CH_3OH); UV (CH_3OH) λ_{max} (log ε) 331 (2.72), 204 (4.19) nm; IR (KBr) ν_{max} 3436, 2927, 1635, 1362, 1048 cm^{-1}; ECD (CH_3OH) λ_{max} ($\Delta\varepsilon$) 348 (+0.25), 304 (−0.06), 252 (+0.42), 213 (−7.54) nm; ^{1}H and ^{13}C NMR data, see Table 3; HRESIMS *m/z* 293.1507 [M − H]$^-$ (calcd for $C_{15}H_{21}N_2O_4$, 293.1507).

Ormosianine E (**5**): colorless oil; $[\alpha]_D^{22}$ +42.2 (*c* 0.08, CH_3OH); UV (CH_3OH) λ_{max} (log ε) 204 (3.95) nm; IR (KBr) ν_{max} 3422, 2930, 1635, 1406, 1173, 992 cm^{-1}; ECD (CH_3OH) λ_{max} ($\Delta\varepsilon$) 259 (+0.48), 228 (+6.79), 195 (−9.94) nm; ^{1}H and ^{13}C NMR data, see Table 3; HRESIMS *m/z* 293.1506 [M − H]$^-$ (calcd for $C_{15}H_{21}N_2O_4$, 293.1507).

Ormosianine F (**6**): colorless oil; $[\alpha]_D^{22}$ −37.1 (*c* 0.09, CH_3OH); UV (CH_3OH) λ_{max} (log ε) 314 (2.79), 204 (4.16) nm; IR (KBr) ν_{max} 3435, 2929, 1632, 1364, 1049 cm^{-1}; ECD (CH_3OH) λ_{max} ($\Delta\varepsilon$) 306 (+0.38), 261 (−0.03), 234 (−1.68), 205 (−6.42) nm; ^{1}H and ^{13}C NMR data, see Table 3; HRESIMS *m/z* 293.1863 [M + H]$^+$ (calcd for $C_{16}H_{25}N_2O_3$, 293.1860).

Ormosianine G (**7**): colorless oil; $[\alpha]_D^{22}$ −22.1 (*c* 0.08, CH_3OH); UV (CH_3OH) λ_{max} (log ε) 205 (4.23) nm; IR (KBr) ν_{max} 3425, 2929, 1629, 1446, 1315, 1170 cm^{-1}; ECD (CH_3OH) λ_{max} ($\Delta\varepsilon$) 232 (+2.25), 205 (−7.78) nm; ^{1}H and ^{13}C NMR data, see Table 3; HRESIMS *m/z* 277.1556 [M − H]$^-$ (calcd for $C_{15}H_{21}N_2O_3$, 277.1558).

Ormosianine H (**8**): colorless oil; $[\alpha]_D^{20}$ −73.3 (*c* 0.10, CH_3OH); UV (CH_3OH) λ_{max} (log ε) 202 (2.97) nm; IR (KBr) ν_{max} 3432, 2934, 1628, 1448, 1169 cm^{-1}; ECD (CH_3OH) λ_{max} ($\Delta\varepsilon$) 230 (−1.13), 209 (+6.05) nm; ^{1}H and ^{13}C NMR data, see Table 4; HRESIMS *m/z* 301.1526 [M + Na]$^+$ (calcd for $C_{15}H_{22}N_2O_3Na$, 301.1523).

Ormosianine I (**9**): colorless oil; $[\alpha]_D^{22}$ −45.9 (*c* 0.10, CH_3OH); UV (CH_3OH) λ_{max} (log ε) 205 (4.13) nm; IR (KBr) ν_{max} 3424, 2921, 1632, 1446, 1115 cm^{-1}; ECD (CH_3OH) λ_{max} ($\Delta\varepsilon$) 232 (+0.88), 205 (−2.65) nm; ^{1}H and ^{13}C NMR data, see Table 4; HRESIMS *m/z* 277.1559 [M − H]$^-$ (calcd for $C_{15}H_{21}N_2O_3$, 277.1558).

Ormosianine J (**10**): colorless oil; $[\alpha]_D^{23}$ −56.8 (*c* 0.09, CH_3OH); UV (CH_3OH) λ_{max} (log ε) 205 (4.05) nm; IR (KBr) ν_{max} 3435, 2929, 1634, 1446, 1117 cm^{-1}; ECD (CH_3OH) λ_{max} ($\Delta\varepsilon$) 228 (+7.58), 202 (+2.46) nm; ^{1}H and ^{13}C NMR data, see Table 4; HRESIMS *m/z* 279.1705 [M + H]$^+$ (calcd for $C_{15}H_{23}N_2O_3$, 279.1703).

Ormosianine K (**11**): colorless oil; $[\alpha]_D^{22}$ −51.6 (*c* 0.09, CH_3OH); UV (CH_3OH) λ_{max} (log ε) 307 (2.91), 204 (2.45) nm; IR (KBr) ν_{max} 3432, 2932, 1633, 1362, 1174 cm^{-1}; ECD (CH_3OH) λ_{max} ($\Delta\varepsilon$) 312 (+0.29), 263 (−0.26), 240 (+0.79), 204 (−6.33) nm; ^{1}H and ^{13}C NMR data, see Table 4; HRESIMS *m/z* 261.1594 [M + H]$^+$ (calcd for $C_{15}H_{21}N_2O_2$, 261.1598).

Ormosianine L (**12**): colorless oil; $[\alpha]_D^{22}$ +68.4 (*c* 0.06, CH_3OH); UV (CH_3OH) λ_{max} (log ε) 310 (3.83), 233 (3.82), 202 (4.09) nm; IR (KBr) ν_{max} 3433, 2938, 1655, 1545, 1494, 1146 cm^{-1}; ECD (CH_3OH) λ_{max} ($\Delta\varepsilon$) 307 (+5.67), 233 (−11.45), 216 (−3.89), 204 (−8.58) nm; ^{1}H and ^{13}C NMR data, see Table 4; HRESIMS *m/z* 259.1440 [M + H]$^+$ (calcd for $C_{15}H_{19}N_2O_2$, 259.1441).

Ormosianine M (**13**): colorless oil; $[\alpha]_D^{22}$ −52.0 (*c* 0.11, CH_3OH); UV (CH_3OH) λ_{max} (log ε) 275 (2.67), 205 (4.00) nm; IR (KBr) ν_{max} 3432, 2932, 1732, 1639, 1245, 1118 cm^{-1}; ECD (CH_3OH) λ_{max} ($\Delta\varepsilon$) 230 (−10.02), 209 (+4.42) nm; ^{1}H and ^{13}C NMR data, see Table 5; HRESIMS *m/z* 323.1969 [M + H]$^+$ (calcd for $C_{17}H_{27}N_2O_4$, 323.1965).

Ormosianine N (**14**): colorless oil; $[\alpha]_D^{22}$ −80.9 (*c* 0.14, CH_3OH); UV (CH_3OH) λ_{max} (log ε) 204 (5.00) nm; IR (KBr) ν_{max} 3433, 2937, 1632, 1448, 1076 cm^{-1}; ECD (CH_3OH) λ_{max} ($\Delta\varepsilon$) 255 (+5.78), 231 (−0.89), 209 (+0.25) nm; ^{1}H and ^{13}C NMR data; see Table 5; HRESIMS *m/z* 265.1911 [M + H]$^+$ (calcd for $C_{15}H_{25}N_2O_2$, 265.1911).

Ormosianine O (**15**): colorless oil; $[\alpha]_D^{22}$ −25.2 (*c* 0.18, CH_3OH); UV (CH_3OH) λ_{max} (log ε) 271 (2.71), 204 (3.86) nm; IR (KBr) ν_{max} 3434, 2933, 1640, 1445, 1160 cm^{-1}; ECD (CH_3OH) λ_{max} ($\Delta\varepsilon$) 265 (+0.36), 235 (+3.92), 292 (−6.38) nm; ^{1}H and ^{13}C NMR data, see Table 5; HRESIMS *m/z* 281.1859 [M + H]$^+$ (calcd for $C_{15}H_{25}N_2O_3$, 281.1860).

Ormosianine P (**16**): white powder; $[\alpha]_D^{20}$ +47.6 (*c* 0.11, CH_3OH); UV (CH_3OH) λ_{max} (log ε) 202 (2.96) nm; IR (KBr) ν_{max} 3430, 2926, 2850, 1576, 1405, 1127 cm^{-1}; ECD (CH_3OH) λ_{max} ($\Delta\varepsilon$) 230 (+2.09), 215 (+1.17), 203 (+1.98) nm; ^{1}H and ^{13}C NMR data, see Table 6; HRESIMS *m/z* 360.2975 [M + H]$^+$ (calcd for $C_{22}H_{38}N_3O$, 360.3009).

ECD Calculation Method. The quantum chemical ECD calculations were performed by Gaussian 16 as previously reported (see details in the Supporting Information).[41,42]

AChE Inhibitory Assay. The acetylcholinesterase inhibitory activity of compounds **1**−**34** was assessed with a modified spectrophotometric method,[43,44] using chlorpyriphos and huperzine A as the positive controls (see details in the Supporting Information).

Molecular Docking Investigation. Molecular docking simulations were achieved employing the software Auto Dock package (http://autodock.scripps.edu/, Molecular Graphics Laboratory at the Department of Molecular Biology, The Scripps Research Institute) as previously described.[44−46] The 3D crystal structure of acetylcholinesterase (PDB code: 1DX4, resolution: 0.375 Å) was obtained from the RCSB Protein Data Bank (https://www.rcsb.org/). The protein was imported into Pymol2.3.0 to remove the water molecule and the original ligands. A grid of 60 × 60 × 60 points in the *x*, *y*, and *z* axes was built centered on the coordinates 34.5 (*x*), 65.1 (*y*), and 9.0 (*z*) near the putative ligand binding site. The number of GA exhaustivenesses was 10 times. The standard 3D structures of compounds **1**, **12**, **13**, and **16**, as well as of positive controls (huperzine A and chlorpyrifos), were constructed based on the above structural elucidations. The resultant complex structures between selected compounds and protein were visualized using the Discovery Studio 4.5 Client.

■ ASSOCIATED CONTENT

Supporting Information

The Supporting Information is available free of charge at https://pubs.acs.org/doi/10.1021/acs.jnatprod.3c00493.

The general experimental procedures, ECD calculation method, biological assay, and original MS and NMR spectra of **1**−**16** (PDF)

■ AUTHOR INFORMATION

Corresponding Author

Xiao-Dong Luo − *State Key Laboratory of Phytochemistry and Plant Resources in West China, Kunming Institute of Botany, Chinese Academy of Sciences, Kunming 650201, People's Republic of China; Yunnan Characteristic Plant Extraction Laboratory, Key Laboratory of Medicinal Chemistry for Natural Resource, Ministry of Education and Yunnan Province, School of Chemical Science and Technology, Yunnan University, Kunming 650500, People's Republic of China;* orcid.org/0000-0002-6768-5679; Phone: +86-0871-65223188; Email: xdluo@mail.kib.ac.cn

https://doi.org/10.1021/acs.jnatprod.3c00493
J. Nat. Prod. 2023, 86, 2193−2205

Authors

Qiong Jin − *State Key Laboratory of Phytochemistry and Plant Resources in West China, Kunming Institute of Botany, Chinese Academy of Sciences, Kunming 650201, People's Republic of China; University of Chinese Academy of Sciences, Beijing 100049, People's Republic of China*

Xu-Jie Qin − *State Key Laboratory of Phytochemistry and Plant Resources in West China, Kunming Institute of Botany, Chinese Academy of Sciences, Kunming 650201, People's Republic of China; University of Chinese Academy of Sciences, Beijing 100049, People's Republic of China*

Wen-Jie Sun − *State Key Laboratory of Phytochemistry and Plant Resources in West China, Kunming Institute of Botany, Chinese Academy of Sciences, Kunming 650201, People's Republic of China; University of Chinese Academy of Sciences, Beijing 100049, People's Republic of China*

Xiao Ding − *State Key Laboratory of Phytochemistry and Plant Resources in West China, Kunming Institute of Botany, Chinese Academy of Sciences, Kunming 650201, People's Republic of China; University of Chinese Academy of Sciences, Beijing 100049, People's Republic of China*

Yun Zhao − *State Key Laboratory of Phytochemistry and Plant Resources in West China, Kunming Institute of Botany, Chinese Academy of Sciences, Kunming 650201, People's Republic of China; University of Chinese Academy of Sciences, Beijing 100049, People's Republic of China*

Chang-Bin Wang − *State Key Laboratory of Phytochemistry and Plant Resources in West China, Kunming Institute of Botany, Chinese Academy of Sciences, Kunming 650201, People's Republic of China; University of Chinese Academy of Sciences, Beijing 100049, People's Republic of China*

Xing-Yu Tao − *State Key Laboratory of Phytochemistry and Plant Resources in West China, Kunming Institute of Botany, Chinese Academy of Sciences, Kunming 650201, People's Republic of China; University of Chinese Academy of Sciences, Beijing 100049, People's Republic of China*

Complete contact information is available at: https://pubs.acs.org/10.1021/acs.jnatprod.3c00493

Author Contributions

[#]Qiong Jin and Xu-Jie Qin contributed equally to this work.

Notes

The authors declare no competing financial interest.

■ ACKNOWLEDGMENTS

The work was financially supported by the High-level Talent Promotion and Training Project of Kunming (2022SCP003), Yunnan Characteristic Plant Screening and R&D Service CXO Platform (2022YKZY001), and Scientific and Technological Innovation Team of Yunnan Province (202105AE160006).

■ REFERENCES

(1) Kinghorn, A. D.; Hussain, R. A.; Robbins, E. F.; Balandrin, M. F.; Stirton, C. H.; Evans, S. V. *Phytochemistry* **1988**, *27*, 439−444.

(2) Herridge, D.; Rose, I. *Field Crop. Res.* **2000**, *65*, 229−248.

(3) Bunsupa, S.; Yamazaki, M.; Saito, K. *Front. Plant Sci.* **2012**, *3*, 239.

(4) Scharnagel, D.; Goller, J.; Deibl, N.; Milius, W.; Breuning, M. *Angew. Chem., Int. Ed.* **2018**, *57*, 2432−2435.

(5) Torres, J.; Escolano, M.; Alzuet-Pina, G.; Sanchez-Rosello, M.; del Pozo, C. *Org. Biomol. Chem.* **2021**, *19*, 8740−8745.

(6) Liu, L.; Alam, M. S.; Hirata, K.; Matsuda, K.; Ozoe, Y. *Pest Manage. Sci.* **2008**, *64*, 1222−1228.

(7) Wink, M.; Hartmann, T.; Witte, L.; Rheinheimer, J. *Z. Naturforsch., C: Biosci.* **1982**, *37C*, 1081.

(8) Zou, J.; Zhao, L.; Yi, P.; An, Q.; He, L.; Li, Y.; Lou, H.; Yuan, C.; Gu, W.; Huang, L.; Hu, Z.; Hao, X. *J. Agric. Food Chem.* **2020**, *68*, 15015−15026.

(9) Villatte, F.; Ziliani, P.; Marcel, V.; Menozzi, P.; Fournier, D. *Pestic. Biochem. Physiol.* **2000**, *67*, 95−102.

(10) Weill, M.; Fort, P.; Berthomieu, A.; Dubois, M. P.; Pasteur, N.; Raymond, M. *Proc. R. Soc. London, Ser. B* **2002**, *269*, 2007−2016.

(11) Fournier, D.; Mutero, A. *Comp. Biochem. Physiol. Part C: Pharmacology, Toxicology and Endocrinology* **1994**, *108*, 19−31.

(12) Grinham, L. R. *Commun. Biol.* **2021**, *4*, 1314.

(13) Wang, X. N.; Wang, Z. J.; Zhao, Y.; Wang, H.; Xiang, M. L.; Liu, Y. Y.; Zhao, L. X.; Luo, X. D. *Nat. Product. Bioprosp.* **2023**, *13*, 10.

(14) Zeng, Q.; Wang, Z. J.; Chen, S.; Wang, H.; Xie, T. Z.; Xu, X. J.; Xiang, M. L.; Chen, Y. C.; Luo, X. D. *Biomed. Pharmacother.* **2022**, *148*, No. 112758.

(15) Yu, H. F.; Ding, C. F.; Zhang, L. C.; Wei, X.; Cheng, G. G.; Liu, Y. P.; Zhang, R. P.; Luo, X. D. *Org. Lett.* **2021**, *23*, 5782−5786.

(16) Zhu, M.; Wang, Z. J.; He, Y. J.; Qin, Y.; Zhou, Y.; Qi, Z. H.; Zhou, Z. S.; Zhu, Y. Y.; Jin, D. N.; Chen, S. S.; Luo, X. D. *J. Ethnopharmacol.* **2021**, *281*, No. 114542.

(17) Le, P. M.; Martin, M. T.; Van Hung, N.; Guenard, D.; Sevenet, T.; Platzer, N. *Magn. Reson. Chem.* **2005**, *43*, 283−293.

(18) Kinghorn, A. D.; Hussain, R. A.; Robbins, E. F.; Balandrin, M. F.; Stirton, C. H.; Evans, S. V. *Phytochemistry* **1988**, *27*, 439.

(19) Nasution, M. P.; Kinghorn, A. D. *Phytochemistry* **1993**, *32*, 1603.

(20) Wysocka, W. *Polym. J. Chem.* **1979**, *53*, 1789.

(21) Torrenegra, R.; Bauereiss, P.; Achenbach, H. *Phytochemistry* **1989**, *28*, 2219.

(22) Ishbaev, A. I.; Aslanov, K. A.; Sadykov, A. S.; Guzenko, T. M. *Khim. Prir. Soedin.* **1974**, *10*, 113.

(23) Muzquiz, M.; Cuadrado, C.; Ayet, G.; de la Cuadra, C.; Burbano, C.; Osagie, A. *J. Agric. Food Chem.* **1994**, *42*, 1447.

(24) Borowiak, T.; Wolska, I.; Wysocka, W.; Brukwicki, T. *J. Mol. Struct.* **2005**, *753*, 27−34.

(25) Keeler, R. F. *J. Toxicol. Environ. Health* **1976**, *1*, 887.

(26) Wink, M.; Meissner, C.; Witte, L. *Phytochemistry* **1995**, *38*, 139.

(27) Lloyd, H. A.; Horning, E. C. *J. Org. Chem.* **1960**, *25*, 1959.

(28) Marinho, L. C.; Carneiro Da Cunha, M. T. M.; Thomas, G.; Barbosa Filho, J. M. *Fitoterapia* **1994**, *65*, 475.

(29) Valenta, Z.; Deslongchamps, P.; Rashid, M. H.; Wightman, R. H.; Wilson, J. S. *Can. J. Chem.* **1966**, *44*, 2525.

(30) Bravo, J. A.; Lavaud, C.; Bourdy, G.; Deharo, E.; Gimenez, A.; Sauvain, M. *Rev. Boliv. Quim.* **2002**, *19*, 12−17.

(31) Torrenegra, R.; Escarria, R.; Bauereiss, P.; Achenbach, H. *Planta Med.* **1985**, *3*, 276−277.

(32) Wang, X.; Lu, Z.; Gomez, A.; Hon, G. C.; Yue, Y.; Han, D.; Fu, Y.; Parisien, M.; Dai, Q.; Jia, G.; Ren, B.; Pan, T.; He, C. *Nature* **2014**, *505*, 117−120.

(33) You, X. J.; Liu, T.; Ma, C. J.; Qi, C. B.; Tong, Y.; Zhao, X.; Yuan, B. F.; Feng, Y. Q. *Anal. Chem.* **2019**, *91*, 10477−10483.

(34) Connolly, G. P.; Duley, J. A. *Trends Pharmacol. Sci.* **1999**, *20*, 218−225.

(35) Lenina, O. A.; Zueva, I. V.; Zobov, V. V.; Semenov, V. E.; Masson, P.; Petrov, K. A. *Sci. Rep.* **2020**, *10*, 16611.

(36) Hansen, R. A.; Gartlehner, G.; Webb, A. P.; Morgan, L. C.; Moore, C. G.; Jonas, D. E. *Clin. Interv. Aging* **2008**, *3*, 211−225.

(37) Vale, A.; Lotti, M. *Handb. Clin. Neurol.* **2015**, *131*, 149−168.

(38) Pan, L.; Sun, J.; Li, Z.; Zhan, Y.; Xu, S.; Zhu, L. *Environ. Sci. Pollut. R.* **2018**, *25*, 4−11.

(39) Jin, Q.; Wei, X.; Qin, X. J.; Gao, F.; Zhu, P. F.; Yuan, H. L.; Njateng, G. S. S.; Dai, Z.; Liu, Y. P.; Luo, X. D. *Fitoterapia* **2020**, *140*, No. 104445.

(40) Jagels, A.; Adpressa, D. A.; Kaweesa, E. N.; McCauley, M.; Philmus, B.; Strother, J. A.; Loesgen, S. *J. Nat. Prod.* **2023**, *86* (7), 1723−1735.

(41) Jin, Q.; Qin, X. J.; Dai, Z.; Zhao, Y.; Zhu, Y. Y.; Chen, S. S.; Liu, Y. P.; Luo, X. D. *Fitoterapia* **2023**, *164*, No. 105356.
(42) Jin, Q.; Zhao, Y. L.; Liu, Y. P.; Zhang, R. S.; Zhu, P. F.; Zhao, L. Q.; Qin, X. J.; Luo, X. D. *J. Ethnopharmacol.* **2022**, *285*, No. 114848.
(43) Yu, M. Y.; Liu, S. N.; Liu, H.; Meng, Q. H.; Qin, X. J.; Liu, H. Y. *Bioorg. Chem.* **2021**, *117*, No. 105404.
(44) Yu, M. Y.; Liu, S. N.; Luo, E. E.; Jin, Q.; Liu, H.; Liu, H. Y.; Luo, X. D.; Qin, X. J. *Phytochemistry* **2022**, *203*, No. 113394.
(45) Yan, X. T.; Chen, J. X.; Wang, Z. X.; Zhang, R. Q.; Xie, J. Y.; Kou, R. W.; Zhou, H. F.; Zhang, A. L.; Wang, M. C.; Ding, Y. X.; Gao, J. M. *J. Nat. Prod.* **2023**, *86* (1), 119−130.
(46) Pagadala, N. S.; Syed, K.; Tuszynski, J. *Biophys. Rev.* **2017**, *9* (2), 91−102.

https://doi.org/10.1021/acs.jnatprod.3c00493
J. Nat. Prod. 2023, 86, 2193−2205